

## UNCERTAINTY EVALUATION OF MULTILATERATION-BASED GEOMETRIC ERROR MEASUREMENT CONSIDERING THE REPEATABILITY OF POSITIONING OF THE MACHINE TOOL

**Xingbao Liu, Yangqiu Xia, Xiaoting Rui**

1) *Institute of Launch Dynamics, Nanjing University of Science and Technology, Nanjing 210094, China*  
(liuxingbao@caep.cn, liuxingbao@caep.cn, ✉ ruixt@163.net)

### Abstract

The sequential multilateration principle is often adopted in geometric error measurement of CNC machine tools. To identify the geometric errors, a single laser tracker is placed at different positions to measure the length between the target point and the laser tracker. However, the measurement of each laser tracker position is not simultaneous and measurement accuracy is mainly subject to positioning repeatability of the machine tool. This paper attempts to evaluate the measurement uncertainty of geometric errors caused by the positioning repeatability of the machine tool and the laser tracker spatial length measurement error based on the Monte Carlo method. Firstly, a direct identification method for geometric errors of CNC machine tools based on geometric error evaluation constraints is introduced, combined with the geometric error model of a three-axis machine tool. Moreover, uncertainty contributors caused by the repeatability of positioning of numerically controlled axes of the machine tool and the laser length measurement error are analyzed. The measurement uncertainty of the geometric error and the volumetric positioning error is evaluated with the Monte Carlo method. Finally, geometric error measurement and verification experiments are conducted. The results show that the maximum volumetric positioning error of the machine tool is 84.1  $\mu\text{m}$  and the expanded uncertainty is 5.8  $\mu\text{m}$  ( $k = 2$ ). The correctness of the geometric error measurement and uncertainty evaluation method proposed in this paper is verified compared with the direct geometric error measurement methods.

Keywords: sequential-multilateration, laser tracker, machine tool, geometric error, measurement uncertainty.

© 2023 Polish Academy of Sciences. All rights reserved

## 1. Introduction

High performance machine tools, especially those with high accuracy, are more and more extensively being used in precision parts machining. However, geometric error seriously deteriorates the machining accuracy of CNC machine tools, on account of basic design and assembly inaccuracies [1]. Geometric error metrology and calibration of CNC machine tools play an important role in accuracy enhancement of machine tools. Therefore, precision instruments are applied

to directly determine geometric errors of moving parts of machine tools, like straight edge, square, and laser interferometer [2]. However, these direct geometric error measurement methods have some disadvantages, such as low measurement efficiency and difficult installation or adjustment of instruments.

Multilateration, constructed with laser trackers, has been long studied towards the volumetric accuracy assessment of CMM or machine tools to reduce the weaknesses of direct measurement methods [3]. By locating laser trackers at different positions of the machine tool table, the position change of the reflector installed at the spindle can be determined according to the length measurement data measured by the tracker, and the geometric error of the machine tool is then identified [4]. Umetsu *et al.* [5] established the measurement coordinate system based on relative position of laser trackers, and determined the geometric errors of the machine tool with the homogeneous coordinate transformation method, Schwenke *et al.* [6] realized the direct solution in the machine tool coordinate system based on the geometric error evaluation constraints and verified its correctness compared with the ball plate method, Wang *et al.* [7] used the theoretical coordinates of the machine tool measured points to determine the position of the laser tracker, but it turned out that the self-calibration process of the tracker position may decrease geometric error measurement accuracy, Wendt *et al.* [8] adopted the laser tracker to directly determine the volumetric positioning error based on the constraints between the commanded points and the actual ones, they improved the measurement accuracy for large-scale workpieces. It is obvious that the core of geometric error measurement using a laser tracker is the measurement algorithm to determine the positions of laser tracker and the geometric errors, and the geometric error evaluation constraint is a good way to achieve high measurement accuracy.

To ensure the effectiveness and the quality of measurement results, the *Monte Carlo method* (MCM) is often used to evaluate the measurement uncertainty in the geometric error measurement of CNC machine tools using the laser tracker. Schwenke *et al.* [9] identified the uncertainty source generated by the length measurement error of the laser tracker and adapted the MCM to evaluate the measurement uncertainty of the machine tool geometric error, Ibaraki *et al.* [10] modeled the uncertainty associated with the length measurement error by systematic and other random errors, and they obtained the uncertainty of machine tool volumetric errors based on the MCM. Aguado *et al.* [11] assessed the measurement environmental noise and laser length measurement error and evaluated the uncertainty of machine tool volumetric position error with the MCM. Liu *et al.* [12] studied the influence of laser tracker length and angle measurement, thermal error and the repeatability of positioning of machine tool, and they improved the geometric accuracy of machine tool with the MCM on uncertainty evaluation. Mutiba *et al.* [13] evaluated uncertainty contributors of spatial displacement measurement and volumetric error uncertainties in the range of micrometers obtained through the MCM. Cong *et al.* [14] optimized the measurement trajectory of multilateration based on the analysis of measurement uncertainty using the MCM, and they found it effective in improving the measurement accuracy of volumetric error measurement. In the configuration of multilateration, commonly only one laser tracker is used at different locations and the machine tool movements are repeated several times at the same points to detect the machine tool geometric error. Consequently, the measurement process can easily become subject to thermal drift and the repeatability of positioning of machine tool. The influence of the repeatability of positioning of machine tool will be greater in the measurement uncertainty evaluation of geometric error, especially when the environment temperature is maintained at  $(20 \pm 0.5)^\circ\text{C}$ .

This paper introduced the direct determination method of geometric error based on evaluating its constraints using a single laser tracker based on sequential multilateration. Secondly, we focus on analyzing uncertainty contributors caused by the positioning repeatability of machine tool

and the spatial length measurement error of the laser tracker, and the results of measuring uncertainty evaluation of geometric error are based on the MCM. The measurement and comparative experiments are carried out to verify the correctness of the method proposed.

## 2. Geometric error modelling

The geometric error model can be established based on the multi-body system kinematics [15]. The kinematic chain of a three-axis CNC machine tool from the workpiece to the cutting tool is the Workpiece-Bed-X axis-Y axis-Z axis-Tool. When we assume that the measurement point of the reflector is placed near the tool center point of the CNC machine tool, the geometric error model can be obtained as follows:

$$\Delta P = C \bullet E, \quad (1)$$

where  $\Delta P = [\Delta X \ \Delta Y \ \Delta Z]^T$ , represents the volumetric error of the tool center point,  $E = [E_{XX}, E_{YX}, E_{ZX}, E_{AX}, E_{BX}, E_{CX}, E_{XY}, E_{YY}, E_{ZY}, E_{AY}, E_{BY}, E_{XZ}, E_{YZ}, E_{ZZ}, E_{A0Z}, E_{B0Y}, E_{C0Y}]^T$  describes the 17 geometric errors of a three-axis machine tool defined in ISO 230-1 [16] and  $C$  is the kinematic model of the machine tool. It can be described as equation (2).

$$C = \begin{bmatrix} 1 & 0 & 0 & 0 & Z & -Y & 1 & 0 & 0 & 0 & Z & 1 & 0 & 0 & 0 & -Z & -Y \\ 0 & 1 & 0 & -Z & 0 & 0 & 0 & 1 & 0 & -Z & 0 & 0 & 1 & 0 & -Z & 0 & 0 \\ 0 & 0 & 1 & Y & 0 & 0 & 0 & 0 & 1 & 0 & 0 & 0 & 0 & 1 & 0 & 0 & 0 \end{bmatrix}, \quad (2)$$

where  $X, Y$  and  $Z$  denote the command coordinates of the machine tool.

The actual position of the measured point is given by:

$$P = P_a + \Delta P. \quad (3)$$

where  $P_a = [X \ Y \ Z]^T$ .

The volumetric positioning error at a certain position of the machine tool is shown in equation (4):

$$\Delta = \sqrt{\Delta X^2 + \Delta Y^2 + \Delta Z^2}. \quad (4)$$

## 3. Measurement algorithm for geometric errors

### 3.1. Geometric error identification based on sequential multilateration

The measurement strategy of multilateration or sequential multilateration is illustrated in Fig. 1. The retroreflector is attached to the machine tool spindle and moves to several command points. The distance between the target and laser tracker is measured and the target position  $P_j$  ( $j = 1, 2, \dots, n$ ) can be determined by the length measured from four or more laser tracker positions  $Q_i$  ( $i = 1, 2, \dots, m$ ) according to equation (5).

$$\begin{cases} \|Q_i - P_j\| = l_{i,j} + l_i \\ \|Q_{i+1} - P_j\| = l_{i+1,j} + l_{i+1} \\ \|Q_{i+2} - P_j\| = l_{i+2,j} + l_{i+2} \\ \|Q_{i+3} - P_j\| = l_{i+3,j} + l_{i+3} \end{cases}, \quad (5)$$

where  $l_i$  stands for the dead length of the laser tracker, for absolute distance measurement,  $l_i$  is 0. The dead length vector of four laser tracker positions can be expressed as  $l_s$ .  $l_{i,j}$  is the displacement recorded by the laser tracker.

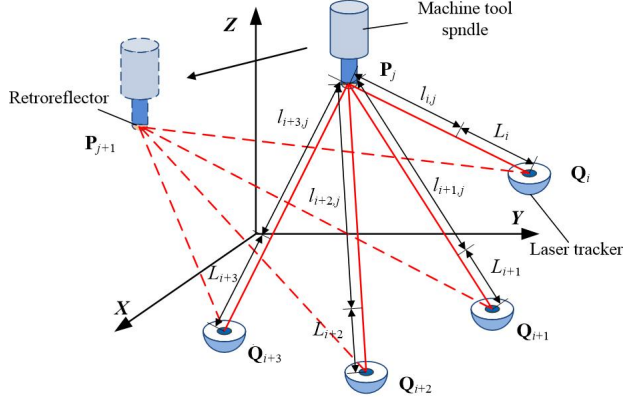


Fig. 1. Configuration of sequential-multilateration using a single laser tracker.

Combining with equation (3), the measurement equation can be written as:

$$\|Q - P_a - C \bullet E\| = l_c + l_s. \quad (6)$$

When the measurement process is completed, the geometric error can be identified by minimizing the sum of squared discrepancies as shown in equation (7):

$$F = \min \sum [\|Q - P_a - C \bullet E\| - l_c - l_s]^2. \quad (7)$$

The minimization problem can be solved with Taylor series expansion and equation (6) can be linearized to the matrix form:

$$J \bullet d = F_d, \quad (8)$$

where  $J$  is the Jacobian matrix of nonlinear equations,  $d$  are the unknown parameters including the position of the laser tracker, 17 geometric errors of a three-axis machine tool, and dead lengths of laser tracker at four positions, and  $F_d$  is a constant matrix.

The positions of the reflector and the laser tracker are both unknown parameters which makes the rank of matrix  $J$  deficient. It cannot be solved using the least square method directly. Therefore, the constraint method is adopted to make matrix  $J$  non-singular. Here are the boundary conditions: straightness errors are 0 at the zero and end positions of the machine tool, angular errors and positioning errors are 0 at the zero position of the machine tool [6], and it can be expressed as:

$$A \bullet d = 0, \quad (9)$$

where  $A$  represents a coefficient matrix of which the diagonal value is 1 corresponding to the constrained geometric errors and other values are 0.

Equation (8) and equation (9) can be merged as:

$$\begin{bmatrix} J \\ A \end{bmatrix} d = \begin{bmatrix} F_d \\ 0 \end{bmatrix}. \quad (10)$$

The iterative method can be used to solve equation (10), like the Levenberg-Marquart method. Finally, geometric errors of the machine tool, coordinates and dead length of the laser trackers can be solved by:

$$\mathbf{d} = \left( \mathbf{M}^T \mathbf{M} + \mu \mathbf{I} \right)^{-1} \mathbf{M}^T \mathbf{G}, \quad (11)$$

where  $\mathbf{M} = [\mathbf{J} \ \mathbf{A}]^T$ ,  $\mathbf{G} = [\mathbf{F}_d \ 0]^T$ ,  $\mu$  is the optimal relaxation factor, and  $\mathbf{I}$  is a unit matrix.

### 3.2. Calculation of initial values for the iterative algorithm

In the process of solving nonlinear equations via the iterative approach, the calculation efficiency and accuracy largely depend on the selection of initial values of unknown parameters. Therefore, this paper presents a simple and fast iterative initial value calculation method which uses the theoretical coordinates of the machine tool to determine the initial value of the positions and dead length of the laser tracker.

#### 3.2.1. Initial values determination of laser tracker positions and dead length

Measurement equation (5) can be converted into equation (12), using the distance equation between the laser tracker position  $\mathbf{Q}_i(x, y, z)$  and the position of measured point  $\mathbf{P}_j(x_j, y_j, z_j)$ :

$$\sqrt{(x - x_j)^2 + (y - y_j)^2 + (z - z_j)^2} = l + l_j, \quad (12)$$

where  $l$  is the dead length of the laser tracker,  $l_j$  is the length indication of the laser tracker when measuring point  $j$ .

The left side and the right side of equation (12) are squared at the same time, which can be transformed into:

$$2xx_j + 2yy_j + 2zz_j + 2ll_j = r + K_j - (l^2 + l_j^2), \quad (13)$$

where  $r = x^2 + y^2 + z^2$ ,  $K_j = x_j^2 + y_j^2 + z_j^2$ .

When  $j = 1$ , equation (13) can be restructured as:

$$2xx_1 + 2yy_1 + 2zz_1 + 2ll_1 = r + K_1 - (l^2 + l_1^2). \quad (14)$$

The difference between equation (14) and equation (13) can be acquired in:

$$2xx_{j1} + 2yy_{j1} + 2zz_{j1} + 2ll_{j1} = K_j - K_1 - l_j^2 + l_1^2, \quad (15)$$

where  $x_{j1} = x_j - x_{11}$ ,  $y_{j1} = y_j - y_{11}$ ,  $z_{j1} = z_j - z_{11}$ ,  $l_{j1} = l_{ji} - l_1$ .

When we subtract equation (13) from other measurement equations, the measurement functions can be written in the matrix form:

$$\mathbf{G}_a \mathbf{L} = \mathbf{h}, \quad (16)$$

where  $\mathbf{G}_a$ ,  $\mathbf{L}$ , and  $\mathbf{h}$  can be given by:

$$\mathbf{G}_a = \begin{bmatrix} x_{21} & y_{21} & z_{21} & l_{21} \\ x_{31} & y_{31} & z_{31} & l_{31} \\ \vdots & \vdots & \vdots & \vdots \\ x_{n1} & y_{n1} & z_{n1} & l_{n1} \end{bmatrix}, \quad (17)$$

$$\mathbf{h} = \frac{1}{2} \begin{bmatrix} K_2 - K_1 - l_2^2 + l_1^2 \\ K_3 - K_1 - l_3^2 + l_1^2 \\ \vdots \\ K_n - K_1 - l_n^2 + l_1^2 \end{bmatrix}, \quad (18)$$

$$\mathbf{L} = [x \quad y \quad z \quad l]^T. \quad (19)$$

Finally, the solution is given by the least square method:

$$\mathbf{L} = (\mathbf{G}_a^T \mathbf{G}_a)^{-1} (\mathbf{G}_a^T \mathbf{h}). \quad (20)$$

### 3.2.2. Selection of initial values for geometric errors

Geometric errors of the machine tool are small values in the micron or micro-radian scale. Therefore, we can set the initial values of the geometric errors to be 0.

## 4. Uncertainty evaluation

The measurement process is to realize the minimization of non-linear equation residuals, which makes it harder to calculate the uncertainty propagation coefficient. Therefore, we use the MCM to evaluate the measurement uncertainty instead of the GUM method.

### 4.1. Measurement uncertainty modelling

We can get the measurement model by the multilateration-based geometric error measurement as follows:

$$\mathbf{D} = [\mathbf{P}_a \quad \mathbf{E} \quad \mathbf{l}_s]^T = f(\mathbf{Q} \quad \mathbf{l}_c). \quad (21)$$

### 4.2. Uncertainty sources and distributions in geometric error measurement

There are two main uncertainty sources for geometric error measurement based on sequential multilateration. One is laser tracker spatial displacement measurement error and the other is repeatability of positioning of the machine tool numerically controlled axes present in Table 1. The machine tool is fixed in a standard environment, in which the temperature, humidity, and isolation are well controlled. It means that the uncertainty sources from the environment are negligible in this paper.

The laser tracker spatial displacement measurement uncertainty contains the length measurement error  $u_{\text{laser\_length}}$ , resolution of laser length  $u_{\text{resolution}}$ , stability of fixed reference sphere  $u_{\text{fixed\_sphere}}$ , and form deviations of reflector  $u_{\text{reflector}}$ . The magnitude of uncertainty sources can be found in the operating manual from the laser tracker manufacturer or reference [17]. A simple approach to estimate the uncertainty of spatial length measurement  $u_l$  using the uncertainty combined method is as follows:

$$u_l = \sqrt{u_{\text{laser\_length}}^2 + u_{\text{resolution}}^2 + u_{\text{reflector}}^2 + u_{\text{fixed\_sphere}}^2}. \quad (22)$$

The uncertainty of repeatability of positioning of numerically controlled axes is evaluated through the measurement of positioning accuracy using a commercial laser interferometer based on the method introduced in ISO 230-2 [18]. We suppose that the distribution of the positioning

Table 1. Uncertainty source and distribution.

Source of uncertainty		Magnitude	Type of distribution
Laser beam	Length measurement error $u_{\text{laser\_length}}, \mu\text{m}$	$0.2 + 0.3l/1000$ ( $k = 2$ ), where $l$ is the measurement length of the laser tracker and the unit of $l$ is millimeter	Gaussian
	Resolution $u_{\text{resolution}}, \text{nm}$	0.5	Rectangular
Stability of the fixed reference sphere $u_{\text{fixed\_sphere}}, \mu\text{m}$		0.1	Rectangular
Optical form deviation of the reflector $u_{\text{reflector}}, \mu\text{m}$		0.03	Rectangular
Repeatability of positioning of numerically controlled axes, $\mu\text{m}$	X	0.8	Rectangular
	Y	0.6	Rectangular
	Z	0.3	Rectangular

repeatability is rectangular. The measurements are repeated ten times to calculate the magnitude of uncertainty and to verify the effectiveness of the assumption of distribution of measurement uncertainty.

#### 4.3. Number of MCM trials and coverage probability

The number of MCM trials is usually more than  $10^6$ . However, a great number of MCM trials means low calculation efficiency and high use of the computing power. Research shows that the uncertainty evaluation error can be guaranteed to be within 5% when the coverage probability is 95% and the number of Monte Carlo trials is  $10^4$ .

#### 4.4. Procedure for the MCM in uncertainty evaluation

There are three dominant steps for geometric error uncertainty evaluation. Firstly, we determine the input of MCM. Secondly, we propagate the *probability density functions* (PDFs) of the input quantities and obtain the probability density function for the output quantity. Finally, we summarize the estimation of the output quantity, the standard uncertainty, and the coverage interval. The detailed procedure of the MCM for uncertainty evaluation of geometric error is given in Fig. 2.

Both the geometric error and volumetric positioning error of machine tool uncertainties can be obtained with the Monte-Carlo method. The expectation of the geometric errors can be derived by equation (23), taken as an estimate of output quantity:

$$\tilde{E}_i = \frac{1}{M} \sum_{r=1}^M E_{ir}, \quad (23)$$

where,  $E_{ir}$  is the  $i_{th}$  geometric error of the three-axis machine tool.

The standard uncertainty can be determined by calculating the standard deviation of the output values as shown in equation (24). Hence the uncertainty of volumetric positioning error can be

derived through equations (1) and (3):

$$u(E_i) = \sqrt{\frac{1}{M-1} \sum_{i=1}^M (E_{ir} - \tilde{E}_i)^2}. \tag{24}$$

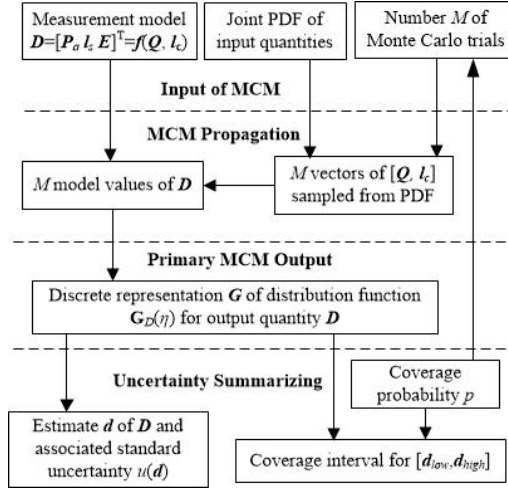


Fig. 2. Flow for geometric error measurement uncertainty evaluation by the MCM.

## 5. Geometric error measurement and uncertainty evaluation experiments

### 5.1. Experimental setup

The geometric error measurement experiments of the linear axes of a five-axis CNC machine tool were carried out at the temperature range of  $(20 \pm 0.5)^\circ\text{C}$ . The machine tool kinematic chain is the same as described in Section 2. The laser tracker was placed at four non-coplanar positions and the machine tool was moved to several positions in turn for detection. During the measurement, the feed rate of the machine tool is 2000 mm/min, and the standstill at each measurement position is 5 s. The geometric error measurement process by the laser tracker is shown in Fig. 3. The coordinates of each position of the laser tracker and the coordinates of the points measured are set as shown in Fig. 4.

After the measurement is finished, the initial values of four laser tracker positions and four dead path lengths are calculated using the algorithm proposed in Section 3, as shown in Table 2.

Table 2. Calculation results of initial values.

Laser tracker	X, mm	Y, mm	Z, mm	L, mm
Position 1	9.285	-643.778	-333.083	-18.309
Position 2	199.886	-655.088	-333.021	-4.898
Position 3	407.639	-625.584	-332.991	11.491
Position 4	408.654	-579.324	-201.116	-24.560



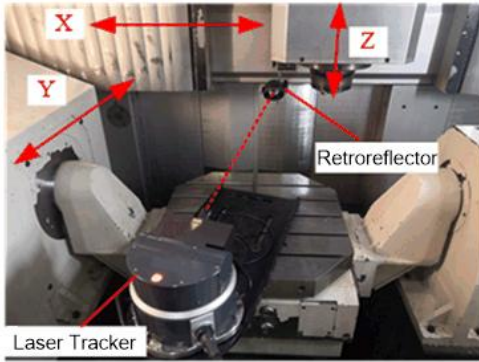


Fig. 3. Geometric error measurement process by laser tracker.

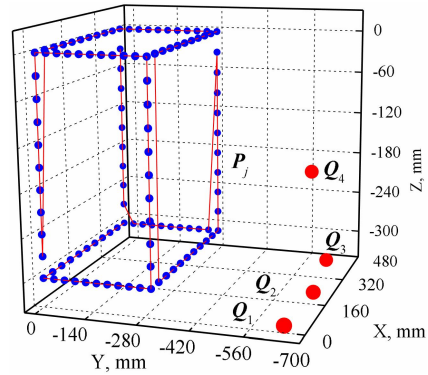


Fig. 4. Laser tracker positions and measured points setting.

## 5.2. Geometric error measurement and uncertainty evaluation results

The Monte-Carlo method is adopted to evaluate the geometric error uncertainty and the volumetric error uncertainty. The number of trials is set to be 10000 and the coverage probability is 95%. The geometric error measurement and uncertainty evaluation results are shown in Table 3. In Table 3,  $E_{hk}$  stands for the linear error motion of  $k$  axis in the direction of  $h$ , where  $h$  and  $k$  can be  $X, Y$  and  $Z$ ,  $E_{xy}$  stands for the angular error motion of  $y$  axis along the direction of  $x$  axis, where  $y$  can be  $A, B$  and  $C$ , and  $x$  can be  $X, Y$  and  $Z$ ,  $E_{A0Z}$  stands for the squareness error between  $Y$  and  $Z$  axis.  $E_{B0Z}$  represents the squareness error of  $X$  and  $Z$  axis, and  $E_{C0X}$  stands for the squareness error between  $X$  and  $Y$  axis.

Table 3. Geometric error measurement and uncertainty evaluation results.

Geometric error	Value	Expanded uncertainty ( $k = 2$ )	Geometric error	Value	Expanded uncertainty ( $k = 2$ )
$E_{XX}, \mu\text{m}$	65.5	3.3	$E_{AY}, \mu\text{m}$	10.6	10.7
$E_{YX}, \mu\text{m}$	3.0	2.1	$E_{BY}, \mu\text{m}$	7.5	11.0
$E_{ZX}, \mu\text{m}$	11.6	3.3	$E_{XZ}, \mu\text{m}$	1.5	1.7
$E_{AX}, \mu\text{rad}$	17.7	7.7	$E_{YZ}, \mu\text{m}$	2.1	2.1
$E_{BX}, \mu\text{rad}$	115.0	8.7	$E_{ZZ}, \mu\text{m}$	8.3	6.9
$E_{CX}, \mu\text{rad}$	27.5	5.6	$E_{A0Z}, \mu\text{rad}$	-106.2	9.3
$E_{XY}, \mu\text{m}$	0.8	2.3	$E_{B0Z}, \mu\text{rad}$	-8.8	12.7
$E_{YY}, \mu\text{m}$	2.6	2.9	$E_{C0Y}, \mu\text{rad}$	116.7	14.8
$E_{ZY}, \mu\text{m}$	3.3	2.8	–	–	–

At the same time, we compare the geometric error evaluation results of the other two methods with the method proposed in this paper. One only considers the laser length measurement error, the other does not take the positioning repeatability of the machine tool into account. The comparative results are shown in Fig. 5.

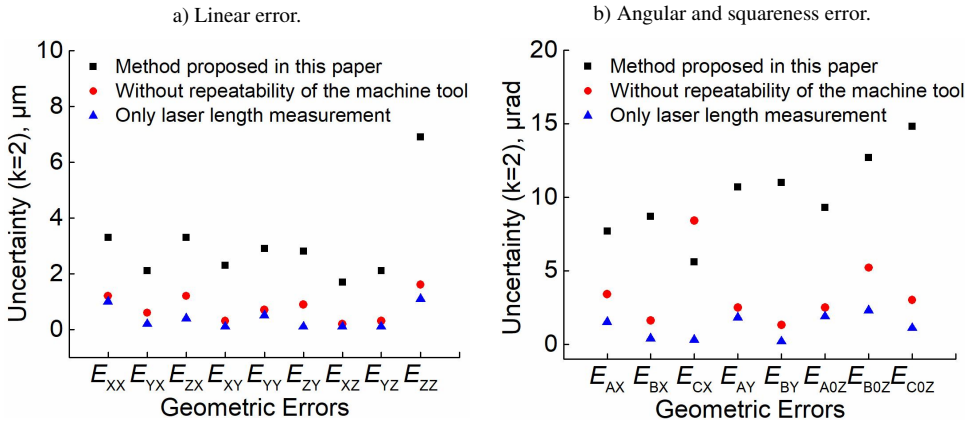


Fig. 5. Comparison of uncertainty evaluation results of geometric errors.

From the comparison diagram of Fig. 5, it can be concluded that the positioning repeatability has a larger influence on the geometric error uncertainty evaluation for the  $E_{ZZ}$ ,  $E_{AX}$ ,  $E_{BX}$ ,  $E_{AY}$ ,  $E_{BY}$  and squareness errors. The impact of machine tool positioning repeatability on geometric error measurement based on sequential multilateration should be considered and actions could be taken to decrease its influence on the measurement results.

### 5.3. Uncertainty evaluation of volumetric positioning error

The measurement uncertainty evaluation results of volumetric positioning error are shown in Fig. 6. The maximum volumetric positioning error measured is 84.1 μm. The expanded measurement uncertainty evaluated with the MCM is 5.8 μm ( $k = 2$ ). Compared with Fig. 5, it is evident that the influence of positioning repeatability of a machine tool on the measurement results of geometric error is much greater than that on the measurement results of volumetric position error. Geometric errors have an “averaging effect” on uncertainty evaluation of volumetric errors.

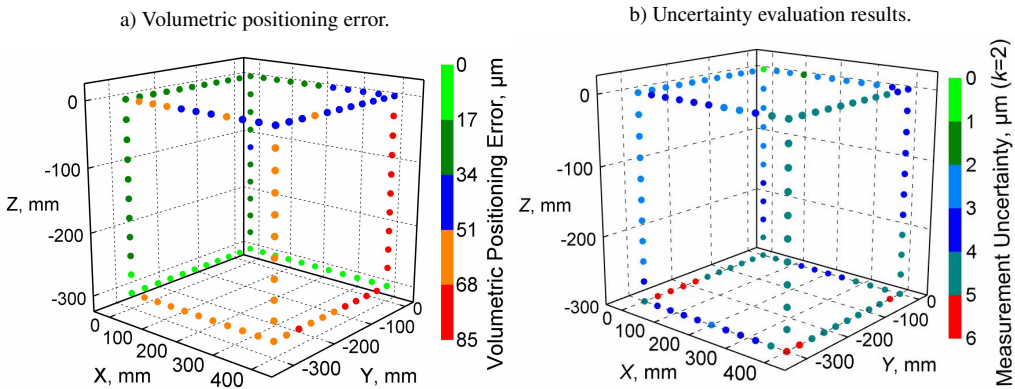


Fig. 6. Uncertainty evaluation results of volumetric positioning errors.

## 6. Verification experiments for the geometric error measurement and uncertainty evaluation method

To verify the effectiveness of the geometric error measurement results, comparative experiments with the traditional direct measurement methods were carried out, and the measurement uncertainties of the measured results are evaluated respectively. The evaluation factor  $H$  for different measurement methods is defined in equation (25). When  $H \leq 1$ , it means that the comparison results are satisfactory and the method proposed is effective.

$$H = \frac{|y_1 - y_2|}{\sqrt{(u^2(y_1) + u^2(y_2))}} \leq 1, \quad (25)$$

where:  $y_1$  is the result measured with the first method and  $u(y_1)$  is the expanded uncertainty of  $y_1$ ,  $k = 2$ ,  $y_2$  is the result measured with the second method, and  $u(y_2)$  is the expanded uncertainty of  $y_2$ ,  $k = 2$ .

### 6.1. Positioning error comparison experiment

An XL80 Renishaw laser interferometer is adopted to detect the positioning error of axes  $X$  and  $Y$ . The measurement uncertainty is evaluated according to the method proposed in ISO 230-2 [17]. The comparative results are drawn in Fig. 7. The maximum difference in positioning deviation of the  $X$  and  $Y$  axes is  $5.3 \mu\text{m}$  and  $3.4 \mu\text{m}$  respectively. The evaluation factor  $H$  is 0.97 and 0.78 respectively, and the comparison result is satisfactory. The evaluation factor of the  $X$ -axis comparison result is larger which may be caused by the environment change when measured by a laser interferometer.

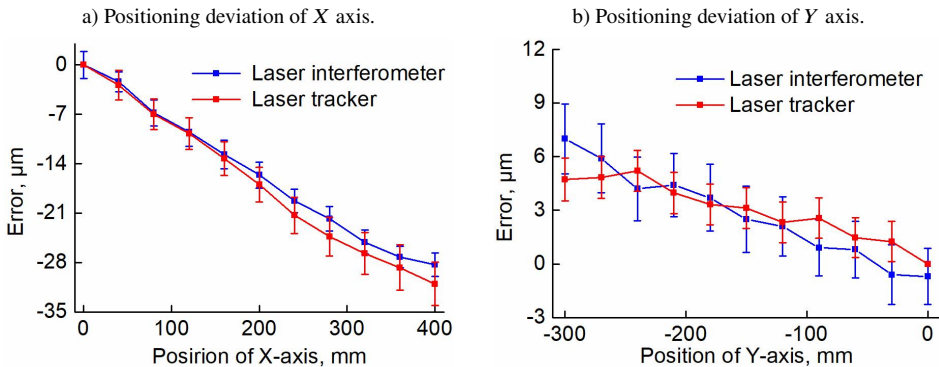


Fig. 7. Comparison results of positioning deviations of X-axis and Y-axis.

### 6.2. Angular deviation comparison experiment

An Agilent laser interferometer was used for angular error measurement. The measurement site and principle are shown in Fig. 8. The angular reflector containing two corner prisms is placed on the machine tool spindle and moves with the axis measured. The beam splitter with a mirror is attached to the machine tool table which is stationary. When the axis measured moves, the optical path variation between the reference beam and the measurement beam can be measured.

Therefore, the angular error can be derived by the optical path variation and the distance between the two corner prisms. The measurement uncertainty is evaluated, and the comparison results are shown in Fig. 9.

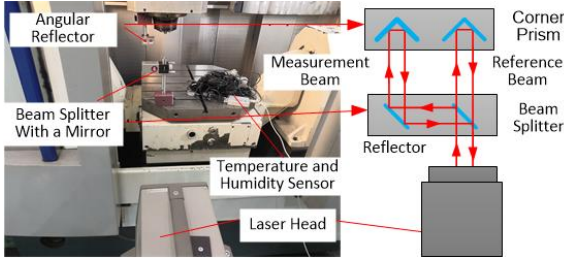


Fig. 8. Angular error measurement by laser interferometer.

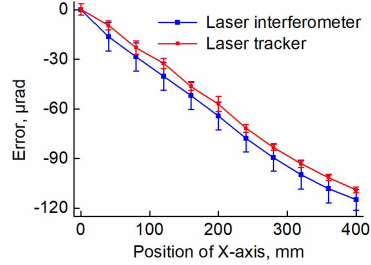


Fig. 9. Comparison results of  $E_{Bx}$ .

It can be seen from Fig. 9 that the trend of measurement results is similar and the maximum difference is  $7.1 \mu\text{rad}$ , the evaluation factor  $H$  is  $0.93$ , *i.e.*, less than 1, and the effectiveness of the experimental results can be verified. However, the evaluation factor is close to 1. Only 17 geometric errors are considered in the measurement process, and the other 4 angular errors are not considered in the geometric error model which still affects the identification results.

### 6.3. Straightness error comparison experiment

The straightness of the Z-axis motion in the YZ plane is measured through a straight edge and an indicator with a resolution of  $0.5 \mu\text{m}$ , and its measurement uncertainty is mainly caused by indication error of indicator, measurement repeatability and straightness of the straight edge. The comparative experimental results are shown in Fig. 10.

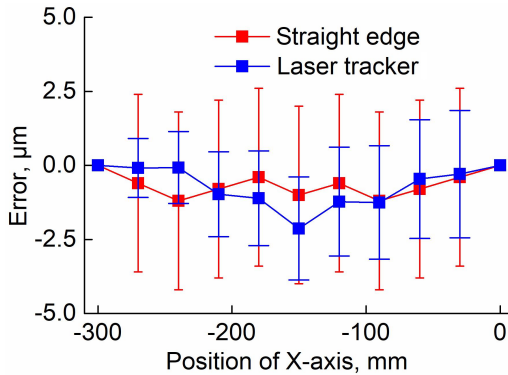


Fig. 10. Comparison results of  $E_{yz}$ .

It can be seen from the Fig. 10 that the maximum difference between the detection results of the two methods is  $1.5 \mu\text{m}$ . The maximum evaluation factor is  $0.21$ , and the comparison results are satisfactory. However, the uncertainty of the traditional measurement method is large, while the measured value is small. In the follow-up, the straight edge with high straightness or flatness can be used for geometric accuracy detection to decrease measurement uncertainty.

#### 6.4. Squareness error comparison experiment

A square and a dial indicator are used to detect the squareness error of  $X$  and  $Y$  axis movements. The detection and comparison results are shown in Table 4. The maximum evaluation factor is 0.67, which proves the correctness of the method proposed in this paper.

Table 4. Results of squareness error comparison.

Squareness error	$E_{C0X}$ , $\mu\text{rad}$	Expanded uncertainty, $\mu\text{rad}$ ( $k = 2$ )
Laser tracker	116.7	14.8
Square and indicator	106	6.2
Evaluation factor $H$	0.67	

### 7. Conclusions

Sequential multilateration is used to measure geometric errors of CNC machine tools using a laser tracker. The geometric error evaluation constraints are adapted to directly obtain the solution of geometric errors, and a simple and linearized method to determine the initial value of the iterative algorithm is given.

The repeatability of the machine tool has a greater impact on the geometric error than the length measurement error. Therefore, when using sequential multiplication, the impact of the repeatability of the machine tool on the geometric error measurement should be considered, and the measurement can be optimized according to the uncertainty analysis results.

Compared with the traditional direct measurement methods, the detection results are similar, and the evaluation factors  $H$  are smaller than 1, which proves the correctness of the method proposed in this paper. However, the geometric error model only contains 17 geometric errors, and the other four geometric errors are not identified. In the future, the modelling can be improved to separate all 21 geometric errors.

#### Acknowledgements

This work was supported by the Basic Technology Research of the State Administration of Science, Technology and Industry for National Defence (J0067-1922-FJC) and by the Major Science and Technology Project of Sichuan Province (2020ZDZX0003).

#### References

- [1] Mannan, M. A., Ramesh, R., & Poo, A. N. (2000). Error compensation in machine tools – a review. Part I: geometric, cutting-force induced and fixture-dependent errors. *Int. Journal of Machine Tools and Manufacture*, 40, 1235–1256. [https://doi.org/10.1016/S0890-6955\(00\)00009-2](https://doi.org/10.1016/S0890-6955(00)00009-2)
- [2] Zongchao, G., Zhen, T., & Xiangqian, J. (2021). Review of geometric error measurement and compensation techniques of ultra-precision machine tools. *Light: Advanced Manufacturing*, 2, 14. <https://doi.org/10.37188/lam.2021.014>
- [3] Muralikrishnan, B., Phillips, S., & Sawyer, D. (2016). Laser trackers for large-scale dimensional metrology: A review. *Precision Engineering*, 44, 13–28. <https://doi.org/10.1016/j.precisioneng.2015.12.001>

- [4] Hughes, E. B., Wilson, A., & Peggs, G. N. (2000). Design of a High-Accuracy CMM Based on Multi-Lateration Techniques. *CIRP Annals – Manufacturing Technology*, 49(1), 391–394. [https://doi.org/10.1016/S0007-8506\(07\)62972-2](https://doi.org/10.1016/S0007-8506(07)62972-2)
- [5] Umetsu, K., Furutnani, R., Osawa, S., Takatsuji, T. & Kurosawa, T. (2005). Geometric calibration of a coordinate measuring machine using a laser tracking system. *Measurement Science & Technology*, 16(12), 2466. <https://doi.org/10.1088/0957-0233/16/12/010>
- [6] Schwenke, H., Franke, M., Hannaford, J., & Kunzmann, H. (2005). Error mapping of CMMs and machine tools by a single tracking interferometer. *CIRP Annals*, 54(1), 475–478. [https://doi.org/10.1016/S0007-8506\(07\)60148-6](https://doi.org/10.1016/S0007-8506(07)60148-6)
- [7] Wang, J., & Guo, J. (2016). Research on the base station calibration of multi-station and time-sharing measurement based on hybrid genetic algorithm. *Measurement*, 94, 139–148. <https://doi.org/10.1016/j.measurement.2016.07.076>
- [8] Wendt, K., Franke, M., & Härtig, F. (2012). Measuring large 3D structures using four portable tracking laser interferometers. *Measurement*, 45(10), 2339–2345. <https://doi.org/10.1016/j.measurement.2011.09.020>
- [9] Schwenke, H., Schmitt, R., Jatzkowski, P., & Warmann, C. (2009). On-the-fly calibration of linear and rotary axes of machine tools and CMMs using a tracking interferometer. *CIRP Annals*, 58(1), 477–480. <https://doi.org/10.1016/j.cirp.2009.03.007>
- [10] Ibaraki, S., Kudo, T., Yano, T., Takatsuji, T., Osawa, S., & Sato, O. (2015). Estimation of three-dimensional volumetric errors of machining centers by a tracking interferometer. *Precision Engineering*, 39, 179–186. <https://doi.org/10.1016/j.precisioneng.2014.08.007>
- [11] Aguado, S., Pérez, P., Albajez, J. A., Velázquez, J., & Santolaria, J. (2017). Monte Carlo method to machine tool uncertainty evaluation. *Procedia Manufacturing*, 13, 585–592. <https://doi.org/10.1016/j.promfg.2017.09.105>
- [12] Liu, Y., Dong, G., & Yong, L. (2015). Volumetric calibration in multi-space in large-volume machine based on measurement uncertainty analysis. *The International Journal of Advanced Manufacturing Technology*, 76 (9–12), 1493–1503. <https://doi.org/10.1007/s00170-014-6367-5>
- [13] Mutilba, U., Yagiüe-Fabra, J. A., Gomez-Acedo, E., Kortaberria, G., & Olarra, A. (2018). Integrated multilateration for machine tool automatic verification. *CIRP Annals*, 555–558. <https://doi.org/10.1016/j.cirp.2018.04.008>
- [14] Cong, H., Zha, J., Li, L., Li, Y., & Chen, Y. (2021). Accuracy evaluation of geometric error calibration using a laser tracer via a formulaic approach. *Measurement Science and Technology*, 32(2), 025003. <https://doi.org/10.1088/1361-6501/abb9e8>
- [15] Rahman, M., Heikkala, J., & Lappalainen, K. (2000). Modeling, measurement and error compensation of multi-axis machine tools. Part I: theory. *International Journal of Machine Tools & Manufacture*, 40(10), 1535–1546. [https://doi.org/10.1016/s0890-6955\(99\)00101-7](https://doi.org/10.1016/s0890-6955(99)00101-7)
- [16] International Organization for Standardization. (2012). *Test code for machine tools, in part 1: geometric accuracy of machines operating under no-load or quasi-static conditions* (ISO Standard No. 230-1:2012). <https://www.iso.org/standard/46449.html>
- [17] Chen, H., Jiang, B., Shi, Z., Sun, Y., Song, H., & Tang, L. (2019). Uncertainty modeling of the spatial coordinate error correction system of the CMM based on laser tracer multi-station measurement. *Measurement Science and Technology*, 30(2), 025007. <https://doi.org/10.1088/1361-6501/aafb1b>

- [18] International Organization for Standardization. (2006). *Test code for machine tools, in Part 2: determination of accuracy and repeatability of positioning numerically controlled axes* (ISO Standard No. 230-2:2006). <https://www.iso.org/standard/35988.html>

**Xingbao Liu** is an on-the-job PhD student at the Institute of Launch Dynamics, Nanjing University of Science & Technology. He specializes in machine tools measurement technology, high-end instrument development and precision manufacturing technology.

**Yangqiu Xia** is an on-the-job PhD student at the School of Mechanical Engineering, Nanjing University of Science & Technology. He specializes in angle measurement technology, ultra-precision machine tool testing technology and development of detection instruments.

**Xiaoting Rui** is an academician at the Chinese Academy of Sciences, director of the Institute of Launch Dynamics, Nanjing University of Science & Technology and a professor at the same university. He specializes in dynamics of multibody systems.